INDIAN JOURNAL OF SCIENCE AND TECHNOLOGY

RESEARCH ARTICLE

Homotopy Analysis Method for an Influence of Dufour-Soret and Melting Process on Magnetohydrodynamic Boundary-Layer Flow towards a Wedge in an Eyring Powell Fluid

K B Umadevi[1], B Patil Mallikarjun[1]*

1 Department of Studies and Research in Mathematics, Tumkur University, Tumakuru572103, Karnataka, India

OPEN ACCESS

Received: 15.12.2021

Accepted: 23-02-2022

Published: 26.04.2022

Citation: Umadevi KB, Mallikarjun BP (2022) Homotopy Analysis Method for an Influence of Dufour-Soret and Melting Process on Magnetohydrodynamic Boundary-Layer Flow towards a Wedge in an Eyring Powell Fluid. Indian Journal of Science and Technology 15(15): 700-711. https://doi.org/10.17485/IJST/v15i16.2354

* **Corresponding author**.

mbp1007@yahoo.com

Funding: K B Umadevi received financial assistance from the "University Grant Commission" under the program of National fellowship for higher education: 201920-NFST-KAR-01277

Copyright: © 2022 Umadevi & Mallikarjun. This is an open access article distributed under the terms of the Creative Commons Attribution License, which permits unrestricted use, distribution, and reproduction in any medium, provided the original author and source are credited.

Published By Indian Society for Education and Environment (iSee)

ISSN
Print: 0974-6846
Electronic: 0974-5645

Abstract

Objectives: The present study investigates the chemical reaction of first-order and Dufour-Soret impact on the magnetohydrodynamic flow of boundary-layer non-Newtonian Eyring Powell fluid across a wedge by taking into account the radiation and melting process. The motion of the fluid is presumed to be incompressible and laminar. Significantly, the presence of the melting process and Dufour-Soret influence the characteristics of mass and heat transfer of the fluid flow. **Methods:** The governing equations are constructed and modified into non-linear, coupled ODEs by utilizing similarity variables and then solved by Homotopy Analysis Method (HAM) based BVPh 2.0 Mathematica package. **Findings:** The velocity, thermal, and concentration profiles are illustrated through graphs and Nusselt number, Sherwood number, and skin-friction coefficient values are shown via tables for varying values of emerging parameters. Results disclosed that the velocity decays with increasing values of fluid parameters (δ, α). It was observed that larger values of Soret parameters (Sr) and Dufour parameter (Dr) increased the concentration and thermal, respectively. It is scrutinized that the velocity suppresses due to extending values of melting parameter (χ). **Novelty:** An incorporation of Soret -Dufour and melting process impact in a non-Newtonian fluid flow across wedge under a magnetic field is novel in the model.

Keywords: Dufour Soret; Eyring Powell fluid; Magnetohydrodynamic; Melting process; Thermal radiation; Wedge

1 Introduction

The flow of a boundary-layer across a wedge is important in recent years due to its numerous applications like geothermal systems, crude oil extraction, heat exchangers, nuclear power plants, as polymer extrusion process, wire drawing, plastic film drawing, production of plastic sheet, metal spinning, friction drag of a ship, etc. The significant aspect of the Eyring Powell fluid is obtained from the kinetic theory of gases relatively

than empirical relations and it reacts like a viscous fluid at larger shear rates. The magnetohydrodynamic boundary-layer flow has been received great interest by its multifarious applications in engineering and technology. Physically, the magnetic fields can bring out the current in an electrically conducting fluid that produced Lorentz's force. A steady fluid flow of a boundary-layer on a stretching /shrinking sheet in a magnetic field was given.[1,2]. An analytical study on entropy analysis on the magnetohydrodynamic flow of boundary-layer across a moving wedge.[3] The steady MHD Newtonian boundary-layer flow towards a stretching sheet with Navier's slip conditions was analytically investigated.[4] An MHD boundary-layer flow past a stretching surface in a micropolar fluid in presence of Joule heating, viscous dissipation, and heat source/sink.[5]

The Dufour-Soret effects play an essential role in the transfer of mass and heat due to its vast applications such as chemical reactors, oil reservoirs, a mixture of gases, binary alloys solidification etc. The transfer of mass caused due to temperature gradient is called Soret [Thermal-Diffusion]. On the other hand, the transfer of heat generated due to concentration gradient is called Dufour [Diffusion-Thermo]. Furthermore, the Dufour-Soret phenomenon has great significant effects on the fluids of very light-weight molecular as well as medium-weight molecular. The two-dimensional unsteady flow of Eyring-Powell magneto nanofluid on a vertical plate under Soret-Dufour impacts.[6]. The mass and heat transfer effect by Soret-Dufour on the sheet in an Eyring-Powell fluid with magnetic dipole and radiation.[7]. An effect of Soret-Dufour over boundary-layer flow due to porous wedge for radiation and suction/injection was studied.[8]. Unsteady flow on a vertical plate within the porous matrix in a micropolar fluid by considering heat absorption, Dufour-Soret, and chemical reaction of first order with an MHD.[9].

The process of transfer of heat due to melting has gained much attention by researchers due to its multifarious applications such as magma solidification, oil extrusion, melting of permafrost, thermal insulation and so on. Moreover, the melting process gives the substance transition from a solid to a liquid state that causes the physical change of the body due to the transfer of heat. An influence of melting process under magnetohydrodynamic flow on a wedge in a Casson nanofluid embedded in the porous stratum.[10] A study on the melting process of nanofluid flow past a wedge with a magnetic field was examined.[11]

An effect of radiation is prominent in controlling the process of heat transfer and it leads to the desired product with a sought quality. The thermal radiation heat transfer has numerous engineering and industrial applications like nuclear plants, aircraft, space vehicles, gas turbines etc. An MHD flow of nanofluid with binary chemical process and radiation was examined.[12]The impact of an aligned magnetic field in a Newtonian fluid with the effects of radiation and Stefan blowing through a stretching/shrinking sheet was examined.[13]. The study presented the heat transfer characteristics of Casson fluid across a stretching curved surface accompanied by thermal radiation and convective boundary conditions under a magnetic field.[14]. HAM is one of the most well-known analytical methods to tackle highly non-linear differential equations. A study by using HAM to tackle the differential equations formulated for the Casson fluid across a porous wedge can be found.[15].

To the extent of our knowledge, no attempts have been made to report the combined impacts of Soret-Dufour and melting process in an electrically-conducting fluid flow due to a wedge analytically as far. Therefore, in this study, we extended the problem of[16] accompanied by the melting process and Soret-Dufour effects. Hence, the present work scrutinized the Dufour-Soret and melting process in boundary-layer magnetohydrodynamic fluid flow in an Eyring Powell across a wedge along with the chemical reaction of first order and radiation. The solutions are obtained analytically by HAM. In addition, an effect of physical parameters like wedge angle parameter, Schmidt number, magnetic parameter, fluid parameters, Prandtl number, Soret and Dufour parameters along the flow was examined. The paper was presented as follows: A mathematical modelling of the problem was given in section 2. The solution procedure and convergence analysis are presented in sections 3 and 4. The graphical representation and discussions are included in section 5. Sections 6 and 7 consist of concluding remarks and references.

2 Mathematical analysis

Consider the laminar boundary-layer flow of non-Newtonian Eyring Powell fluid through the wedge. The velocity components (u, v)along with cartesian coordinates (x, y) are shown in Figure 1 in horizontal and vertical directions, respectively. Let x and y axis was taken surface of wedge, respectively. Let $U(x) = ax^b$is free stream velocity where, a is constant. The uniform-magnetic field B_0 is measured along the y - direction.

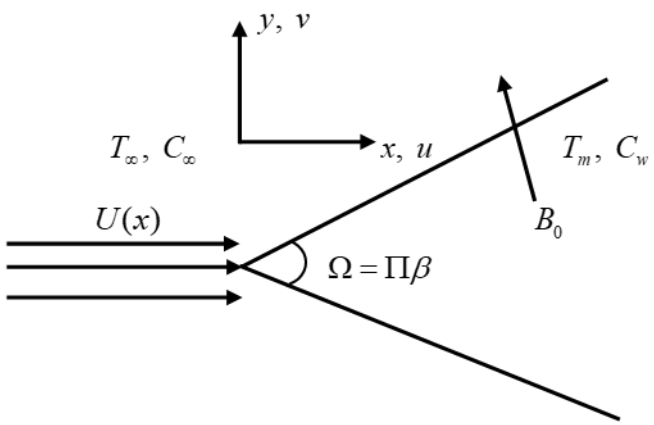

Fig 1. Diagram of the flow across a wedge

Based on the assumptions made above, the governing boundary-layer flow equations are defined as given below,

$$\frac{\partial u}{\partial x}+\frac{\partial v}{\partial y}=0 \tag{1}$$

$$\frac{\partial u}{\partial x}u+\frac{\partial u}{\partial y}v=U\frac{dU}{dx}+\frac{\partial^2 u}{\partial y^2}\left(v+\frac{1}{\rho\varepsilon\gamma}\right)-\frac{1}{2\rho\varepsilon\gamma^3}\left(\frac{\partial u}{\partial y}\right)^2\quad\frac{\partial^2 u}{\partial y^2}-\frac{\sigma B_0^2}{\rho}(u-U) \tag{2}$$

$$\frac{\partial T}{\partial x}u+\frac{\partial T}{\partial y}v=\frac{\kappa}{\rho C_P}\frac{\partial^2 T}{\partial y^2}+\frac{D_P K_T}{C_P C_S}\frac{\partial^2 C}{\partial y^2}+\frac{16\hat{\sigma}T_\infty^3}{3\rho\hat{K}C_P}\frac{\partial^2 T}{\partial y^2} \tag{3}$$

$$\frac{\partial C}{\partial x}u+\frac{\partial C}{\partial y}v=D_P\frac{\partial^2 C}{\partial y^2}+\frac{D_P K_T}{T_m}\frac{\partial^2 T}{\partial y^2} \tag{4}$$

boundary constraints are,

$$\begin{aligned} &y=0;\quad u=0,\quad T=T_m,\quad C=C_w,\\ &y\to\infty;\quad u=U,\quad T\to T_\infty,\quad C\to C_\infty, \end{aligned} \tag{5}$$

and

$$\left(\frac{\partial T}{\partial y}\right)_{y=0}=\frac{\rho v(x,0)}{\kappa}\left[A+(T_m-T_0)C_S\right] \tag{6}$$

Here $\nu,\rho,$ and $\sigma$are viscosity coefficient, fluid density, and electrical conductivity, ε and γ are the fluid material parameters, κ is thermal conductivity, $\hat{\sigma}$ is Stefan-Boltzmann constant, C_P is constant pressure with specific heat, D_P is diffusion coefficient, T_∞ is free-stream temperature, $\hat{K}$ is mean absorption coefficient, A is the fluid latent heat, C_s is concentration susceptibility, C_∞ is free-stream concentration, T_o is solid surface temperature, K_T is the thermal diffusion coefficient and T_m is melting temperature.

The following similarity transformations will be introduced as follows;

$$\eta=x^{\frac{-(1-b)}{2}}y\sqrt{\frac{(b+1)a}{2v}},\quad \psi=x^{\frac{1+b}{2}}\sqrt{\frac{2av}{(b+1)}},\quad \phi(\eta)=\frac{C-C_\infty}{C_w-C_\infty},\text{ and }\quad \theta(\eta)=\frac{T-T_m}{T_\infty-T_m} \tag{7}$$

Here, ψ and η are stream function and similarity variables, respectively.

The stream function satisfies the continuity equation (1) such that;

$$u=\frac{\partial\psi}{\partial y},\quad\text{and}\quad v=-\frac{\partial\psi}{\partial x}$$

By using Eq. (7) into Eqs. (2)-(6) takes the form;

$$\frac{d^3f}{d\eta^3}(1+\delta)+\frac{d^2f}{d\eta^2}f(\eta)+\left(1-\left(\frac{df}{d\eta}\right)^2\right)\beta-\left(\frac{d^2f}{d\eta^2}\right)^2\left(\frac{1}{2-\beta}\right)\frac{d^3f}{d\eta^3}\delta\alpha-M\left(\frac{df}{d\eta}-1\right)(2-\beta)=0 \tag{8}$$

$$(1+Ra)\frac{d^2\theta}{d\eta^2}+f(\eta)\frac{d\theta}{d\eta}\Pr+\frac{d^2\phi}{d\eta^2}Dr\Pr=0 \tag{9}$$

$$\frac{d^2\phi}{d\eta^2}+Scf(\eta)\frac{d\phi}{d\eta}+Sc\frac{d^2\theta}{d\eta^2}Sr=0 \tag{10}$$

$$\begin{gathered}\frac{df}{d\eta}(0)=0,\quad \theta(0)=1,\quad \phi(0)=1\\ \frac{df}{d\eta}(\infty)\to 1,\quad \theta(\infty)\to 0,\quad \phi(\infty)\to 0\end{gathered} \tag{11}$$

and

$$f(0)\Pr+\chi\frac{d\theta}{d\eta}(0)=0 \tag{12}$$

where, $\delta=\frac{1}{\mu\varepsilon\gamma}$and $\alpha=\frac{a^3x^{3b-1}}{3\gamma^2v}$; Eyring Powell fluid parameters, $\beta=\frac{2b}{1+b}$; wedge angle parameter, $\Pr=\frac{\mu C_P}{\kappa}$; Prandtl number, $M=\frac{\sigma B_0^2x^{1-b}}{\rho a}$; magnetic parameters, $Ra=\frac{16\hat{\sigma}T_\infty^3}{3\hat{K}\kappa}$;Radiation parameter, $S_c=\frac{D_P}{v}$;Schmidt number, $Dr=\frac{D_PK_t}{C_PC_Sv}\left(\frac{C_w-C_\infty}{T_w-T_\infty}\right)$;Dufour number, $Sr=\frac{D_PK_t}{T_PV}\left(\frac{T_w-T_\infty}{C_w-C_\infty}\right)$;Soret number, and $\chi=\frac{C_P(T_\infty-T_m)}{A+C_S(T_m-T_0)}$; melting parameter.

The coefficient of skin-friction, Nusselt number and Sherwood number are written as;

$$\hat{C}_f=\frac{\tau_w}{U^2\rho},\quad \hat{N}u_x=\frac{q_wx}{\kappa(T_W-T_m)},\quad \text{and}\quad \hat{S}h_x=\frac{m_wx}{D_p(C_\infty-C_W)} \tag{13}$$

where τ_w, m_w, and q_w are shear stress, mass flux, and heat flux given as follows,

$$\tau_w=\left(\mu+\frac{1}{\varepsilon\gamma}\right)\left(\frac{\partial u}{\partial y}\right)_{y=0}-\frac{1}{6\gamma^3\varepsilon}\left(\frac{\partial u}{\partial y}\right)^3_{y=0},\quad q_w=-\left(\kappa+\frac{16\hat{\sigma}T_\infty^3}{3\hat{K}}\right)\left(\frac{\partial T}{\partial y}\right)_{y=0},\text{ and}\quad m_w=-D_p\left(\frac{\partial C}{\partial y}\right)_{y=0} \tag{14}$$

By Eqs. (7) and (14) in Eq. (13) becomes,

$$\widehat{R}_x^{-1/2}\widehat{N}u_x=-\sqrt{\frac{1+b}{2}}(1+Ra)\frac{d\theta}{d\eta}(0),\quad \text{and}\quad \widehat{\mathrm{Re}_x^{-1/2}}\widehat{S}h_x=-\sqrt{\frac{1+b}{2}}\frac{d\phi}{d\eta}(0) \tag{15}$$

Here, $\hat{R}_{e_x}=\frac{Ux}{v}$is the Reynolds number.

3 Methodology

Shijun Liao 1992 introduced an analytical method called the Homotopy Analysis Method to tackle non-linear differential equations. The system of Eqs. (8)-(10) along with (11) and (12) are solved by utilizing HAM by choosing appropriate linear operators and initial guesses are as follows,

$$L_1(f)=-\left(\frac{df}{d\eta}-\frac{d^3f}{d\eta^3}\right) \tag{16}$$

$$L_2(\theta)=-\left(\theta-\frac{d^2\theta}{d\eta^2}\right) \tag{17}$$

$$L_2(\phi)=-\left(\phi-\frac{d^2\phi}{d\eta^2}\right) \tag{18}$$

with the properties;

$$L_1\left(c_1+c_2e^{\eta}+c_3e^{-\eta}\right) \tag{19}$$

$$L_2\left(c_4e^{\eta}+c_5e^{-\eta}\right) \tag{20}$$

$$L_3\left(c_6e^{\eta}+c_7e^{-\eta}\right) \tag{21}$$

Here, C_1-C_7 are arbitrary constants and initial guesses as below,

$$f_0(\eta)=\eta-[1-e^{-\eta}]-\frac{\chi}{\Pr} \tag{22}$$

$$\theta_0(\eta)=e^{-\eta} \tag{23}$$

$$\phi_0(\eta)=e^{-\eta} \tag{24}$$

Let $\hat{q}\in[0,1]$ as an embedding parameter, h_1, h_2 and h_3 as non-zero convergence control parameters, we can develop a deformation equation of zeroth-order as follows,

$$L_1\left[\tilde{f}(\eta,\hat{q})-f_0(\eta)\right](1-\hat{q})=N_1[\tilde{f}(\eta,\hat{q})]\hat{q}h_1 \tag{25}$$

$$L_2\left[\tilde{\theta}(\eta,\hat{q})-\theta_0(\eta)\right](1-\hat{q})=N_2[\tilde{\theta}(\eta,\hat{q}),\tilde{f}(\eta,\hat{q}),\tilde{\phi}(\eta,\hat{q})]\hat{q}h_2 \tag{26}$$

$$L_3\left[\tilde{\phi}(\eta,\hat{q})-\phi_0(\eta)\right](1-\hat{q})=N_3[\tilde{\phi}(\eta,\hat{q}),\tilde{\theta}(\eta,\hat{q}),\tilde{f}(\eta,\hat{q})]\hat{q}h_3 \tag{27}$$

where, N_1, N_2, and N_3 are nonlinear operators chosen below,

$$\begin{aligned}N_1[\tilde{f}(\eta,\hat{q})]=&\frac{\partial^3 f(\eta,\hat{q})}{\partial\eta^3}(1+\delta)+\frac{\partial^2 f(\eta,\hat{q})}{\partial\eta^2}f(\eta,\hat{q})+\beta\left(1-\left(\frac{\partial f(\eta,\hat{q})}{\partial\eta}\right)^2\right)-\left(\frac{1}{2-\beta}\right)\left(\frac{\partial^2 f(\eta,\hat{q})}{\partial\eta^2}\right)^2\\&\frac{\partial^3 f(\eta,\hat{q})}{\partial\eta^3}\delta\alpha-(2-\beta)M\left(\frac{\partial f(\eta,\hat{q})}{\partial\eta}-1\right)\end{aligned} \tag{28}$$

$$N_2[\tilde{\theta}(\eta,\hat{q}),\tilde{f}(\eta,\hat{q}),\quad\tilde{\phi}(\eta,\hat{q})]=(1+Ra)\frac{\partial^2\theta(\eta,\hat{q})}{\partial\eta^2}+\frac{\partial\theta(\eta,\hat{q})}{\partial\eta}\Pr f(\eta,\hat{q})+Dr\frac{\partial^2\phi(\eta,\hat{q})}{\partial\eta^2}\Pr \tag{29}$$

$$N_3[\tilde{\phi}(\eta,\hat{q}),\tilde{\theta}(\eta,\hat{q}),\tilde{f}(\eta,\hat{q})]=\frac{\partial^2\phi(\eta,\hat{q})}{\partial\eta^2}+\frac{\partial\phi(\eta,\hat{q})}{\partial\eta}Scf(\eta,\hat{q})+Sr\frac{\partial^2\theta(\eta,\hat{q})}{\partial\eta^2}Sc \tag{30}$$

subject to boundary constraints,

$$\frac{\partial\hat{f}(0,\hat{q})}{\partial\eta}=0,\quad\hat{\theta}(0,\hat{q})=\hat{\phi}(0,\hat{q})=1 \tag{31}$$

$$\frac{\partial\hat{f}(\infty,\hat{q})}{\partial\eta}=1,\quad\hat{\theta}(\infty,\hat{q})=\hat{\phi}(\infty,\hat{q})=0 \tag{32}$$

and

$$\hat{f}(0,\hat{q})\Pr+\chi\frac{\partial\theta(0,\hat{q})}{\partial\eta}=0 \tag{33}$$

If $\hat{q}=1,$ and $\hat{q}=0$we get,

$$\hat{f}(\eta;1)=f(\eta)\quad\hat{f}(\eta;0)=f_0(\eta) \tag{34}$$

$$\hat{\theta}(\eta;1)=\theta(\eta)\quad\hat{\theta}(\eta;0)=\theta_0(\eta) \tag{35}$$

$$\hat{\phi}(\eta;1)=\phi(\eta)\quad\hat{\phi}(\eta;0)=\phi_0(\eta) \tag{36}$$

and using Taylor's series w. r. t.

$$\hat{f}(\eta;\hat{q}) = f_0(\eta) + \sum_{r=1}^{\infty} \hat{q}^r f_r(\eta) \tag{37}$$

$$\hat{\theta}(\eta;\hat{q}) = \theta_0(\eta) + \sum_{r=1}^{\infty} \hat{q}^r \theta_r(\eta) \tag{38}$$

$$\hat{\phi}(\eta;\hat{q}) = \phi_0(\eta) + \sum_{r=1}^{\infty} \hat{q}^r \phi_r(\eta) \tag{39}$$

where,

$$f_r(\eta) = \left(\frac{1}{r!}\right) \frac{\partial^r f(\eta,\hat{q})}{\partial \hat{q}^r}\bigg|_{\hat{q}=0} \tag{40}$$

$$\theta_r(\eta) = \left(\frac{1}{r!}\right) \frac{\partial^r \theta(\eta,\hat{q})}{\partial \hat{q}^r}\bigg|_{\hat{q}=0} \tag{41}$$

$$\phi_r(\eta) = \left(\frac{1}{r!}\right) \frac{\partial^r \phi(\eta,\hat{q})}{\partial \hat{q}^r}\bigg|_{\hat{q}=0}. \tag{42}$$

The series Eqs. (37)-(39) are converging hence the solution of the series is obtained as follows,

$$\hat{f}(\eta;p) = f_0(\eta) + \sum_{r=1}^{\infty} f_r(\eta) \tag{43}$$

$$\hat{\theta}(\eta;p) = \theta_0(\eta) + \sum_{r=1}^{\infty} \theta_r(\eta) \tag{44}$$

$$\hat{\phi}(\eta;p) = \phi_0(\eta) + \sum_{r=1}^{\infty} \phi_r(\eta) \tag{45}$$

The deformation equations of r^{th} order become,

$$L_1\left[f_r(\eta) - \Delta_r f_{r-1}(\eta)\right] = h_1 R_r^f(\eta) \tag{46}$$

$$L_2\left[\theta_r(\eta) - \Delta_r \theta_{r-1}(\eta)\right] = h_2 R_r^{\theta}(\eta) \tag{47}$$

$$\begin{gathered} L_3\left[\phi_r(\eta) - \Delta_r \phi_{r-1}(\eta)\right] = h_3 R_r^{\phi}(\eta) \\ f_r'(0) = 0, \quad \theta_r(0) = \phi_r(0) = 1 \end{gathered} \tag{48}$$

$$f_r'(\infty) = 1, \quad \theta_r(\infty) = \phi_r(\infty) = 0, \tag{49}$$

and

$$f_r(0)\,\mathrm{Pr} + \chi\theta_r'(0) = 0 \tag{50}$$

where,

$$\begin{aligned} R_r^f(\eta) = f_{r-1}'''(1+\delta) + \sum_{k=0}^{r-1} f_k'' f_{r-1-k} + \beta\left(1 - \sum_{k=0}^{r-1} f_{r-1-k}' f_k'\right) - \left(\frac{1}{2-\beta}\right)\delta\alpha \sum_{k=0}^{r-1} f_{r-1-k}''' f_{r-1-k} \sum_{i=0}^{k} f_{k-i}'' f_k'' \\ - M(2-\beta)\left(f_{r-1}' - 1\right) \end{aligned} \tag{51}$$

$$R_r^{\theta}(\eta) = \theta_{r-1}''(1+Ra) + \mathrm{Pr}\sum_{k=0}^{r-1} \theta_k' f_{r-1-k} + \mathrm{Pr}\,\phi_{r-1}'' Dr \tag{52}$$

$$R_r^{\phi}(\eta) = \phi_{r-1}'' + Sc\sum_{k=0}^{r-1} f_{r-1-k}\phi_k' + SrSc\theta_{r-1}'' \tag{53}$$

$$\Delta_r = \begin{cases} 1, & r > 1 \\ 0, & r \leq 1 \end{cases} \tag{54}$$

The general solutions of Eqs. (46)-(48) are given by,

$$f_r(\eta) = \hat{f}_r(\eta) + c_1 + c_2 e^{\eta} + c_3 e^{-\eta} \tag{55}$$

$$\theta_r(\eta) = \hat{\theta}_r(\eta) + c_4 e^{\eta} + c_5 e^{-\eta} \tag{56}$$

$$\phi_r(\eta) = \hat{\phi}_r(\eta) + c_6 e^{\eta} + c_7 e^{-\eta} \tag{57}$$

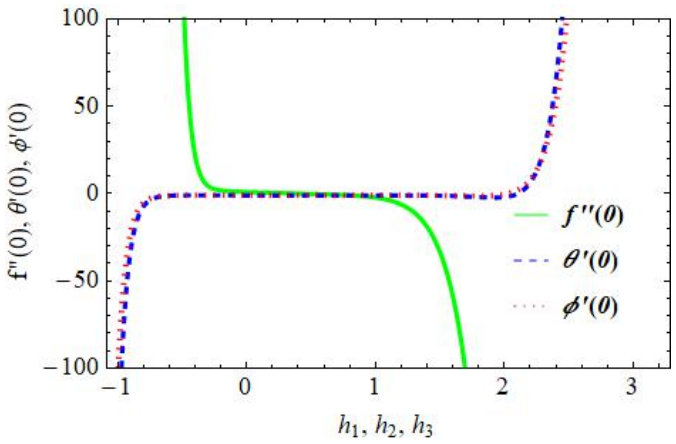

Fig 2. The h_1, h_2, and h_3 curves w. r. t. $f''(0), \theta'(0)$, and $\phi'(0)$.

4 Convergence analysis

Figure 2 is plotted for proper values of the auxiliary parameter from the valid domain. From these figures, the series convergence of the domain was [-0.4, 1], [-0.6, 1.6], and [-0.7, 1.7] for h_1, h_2 and h_3 respectively.

5 Results and discussion

The Eqs. (9)-(11) accompanied by the boundary constraints (12) and (13) are coupled and nonlinear which are tackled by HAM. The velocity, thermal, and concentration are plotted in Figures 3, 4, 5, 6, 7, 8, 9 and 10 for constant values of controlling parameters like $\alpha = 1, \delta = 0.4, M = 1, \beta = 1.5, \Pr = 6, \quad Sc = 4, \quad Dr = 0.2, \quad \chi = 0.4, \quad Ra = 0.5$and $Sr = 0.3$. The skin-friction, Sherwood number, and Nusselt number values are shown via Tables 1 and 2 .

An influence of α and δ along velocity distribution is shown in Figures 3 and 4. The velocity distributions in Figures 3 and 4 are suppressed with increasing values of α and δ. For increasing δ the fluid viscosity i.e.,μdecays, which causes a decrease in fluid velocity. This result was agreed well with [16]. The skin friction is enhanced and suppressed for larger α and δ respectively as demonstrated in Table 1. Figure 5 reflects the impact of M on velocity field. The velocity increases with the extending values of M. The raising in values of magnetic parameter generates a Lorentz force which leads to the movement of particles causes to intensify the velocity. Table 1 shows that an increasing M develops the skin friction. The effect of β along velocity profile is sketched in Figure 6. This plot exhibits that various values of β, velocity grow up. Physically, β which represents a pressure gradient; therefore, $\beta > 0$ showing a favourable pressure gradient that increases the flow of fluid within the boundary, further $\beta < 0$ indicating an unfavourable pressure gradient. For larger values of β intensifies the coefficient of skin friction. The results obtained for M and B in the present study was well agreement with [10].

The effect of Ra on temperature distribution is shown in Figure 7. The figure represents that for larger Ra the thermal field enhances. The Sherwood and Nusselt numbers for varying values show the decreased and increased behaviour, respectively. Figures 8 and 9 exemplify the influence of Dr on temperature and Sr on concentration. An enhance in values of Dr increases the thermal profile. A larger value of Dr enhances the heat of the system leads to temperature growing up. A concentration profile rises for larger values of Sr Physically, the Dufour number is the ratio of the concentration difference to temperature difference and vice versa for the Soret number. An increasing value of Dr both the Sherwood and Nusselt numbers were decayed. The Nusselt number was constant and the Sherwood number decreased with larger values of Sr is observed in Table 2. The impact of χon velocity is plotted in Figure 10. For larger χ, decays the velocity distribution. Increase χ which will enhance the melting intensity and hence causes the velocity to decrease and this result was consent to the work done by [15]. The Sherwood and Nusselt numbers were enhanced with increasing values of χ.

6 Conclusion

The effects of Dufour-Soret and melting process on magnetohydrodynamic laminar flow of boundary-layer Eyring Powell fluid through a wedge subjected to binary chemical reaction and radiation were analysed. The boundary constraints account the melting process used at the surface which causes the fluid to accelerate. Governing equations are converted into coupled,

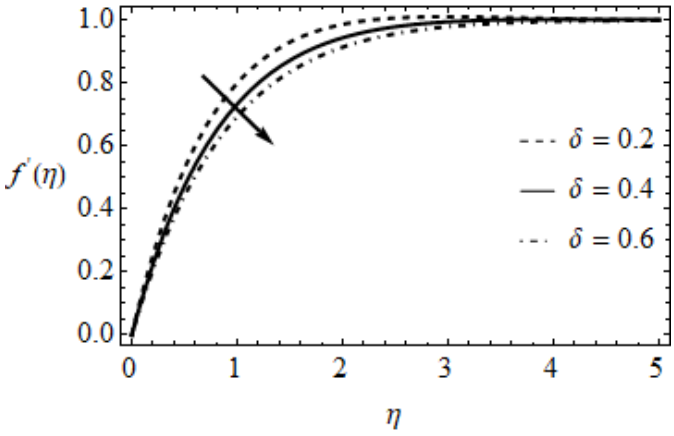

Fig 3. The variation of δ w.r.t. $f'(\eta)$

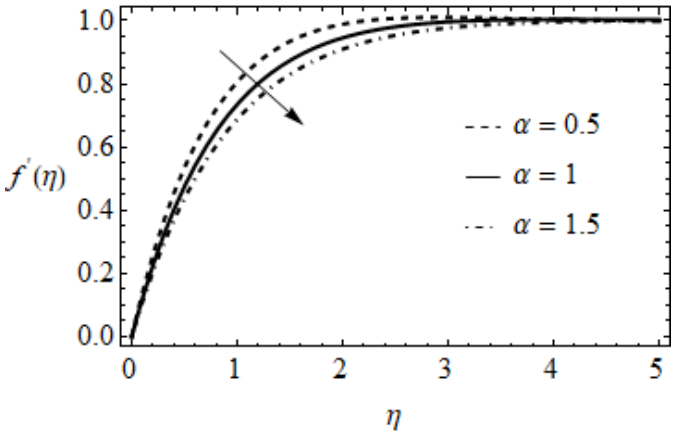

Fig 4. The variation of α W.r.t. $f'(\eta)$

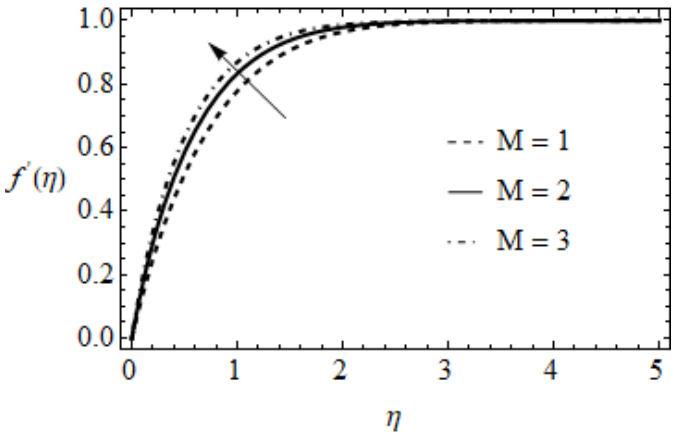

Fig 5. The variation of M w. r. t. $f'(\eta)$

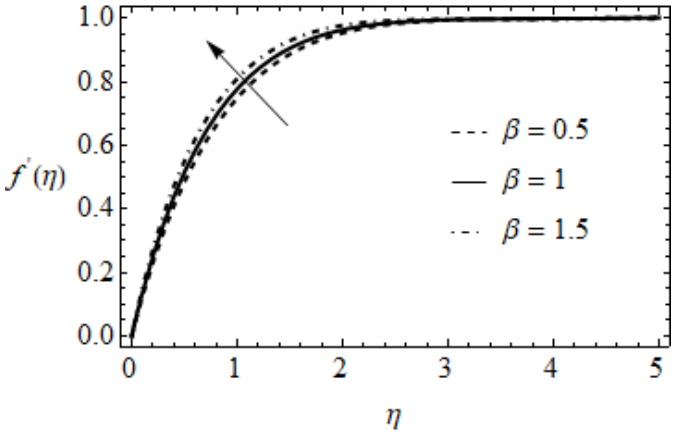

Fig 6. The variation of β w. r. t. $f'(\eta)$

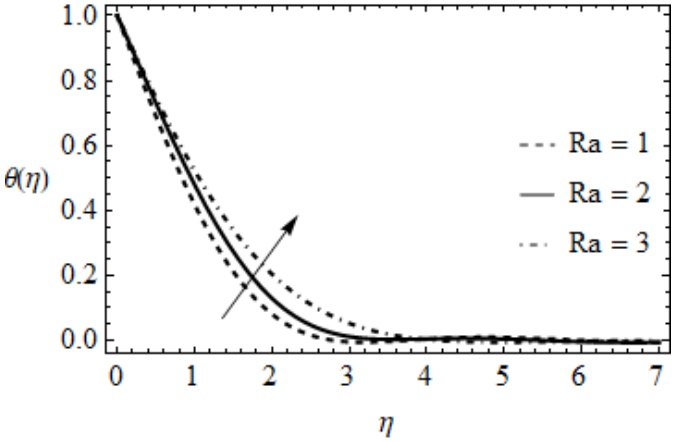

Fig 7. The variation of Ra w.r. t. $\theta(\eta)$.

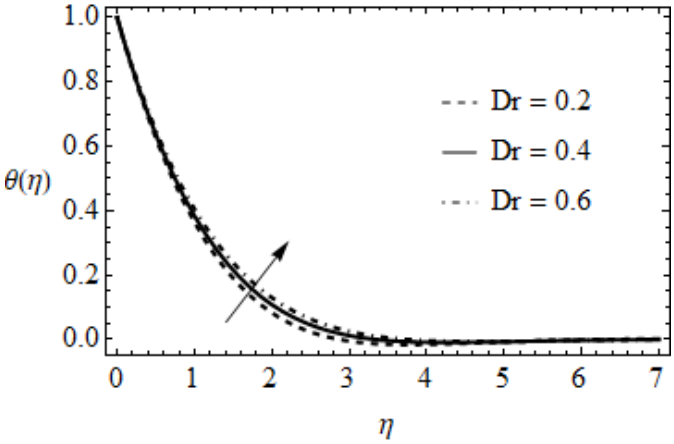

Fig 8. The variation of Dr w. r.t. $\theta(\eta)$

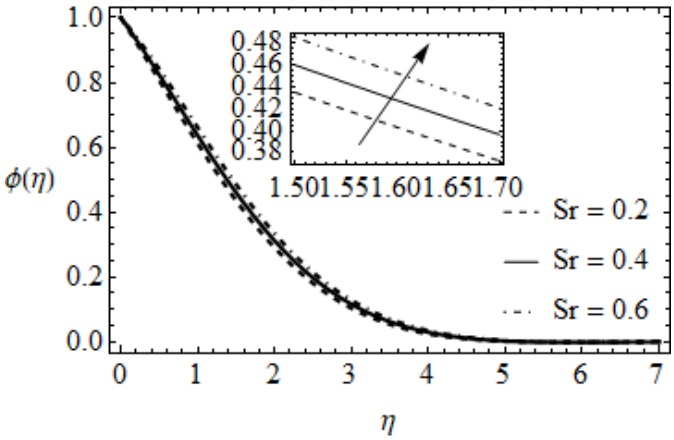

Fig 9. The variation of Sr w.r.t. $\phi(\eta)$

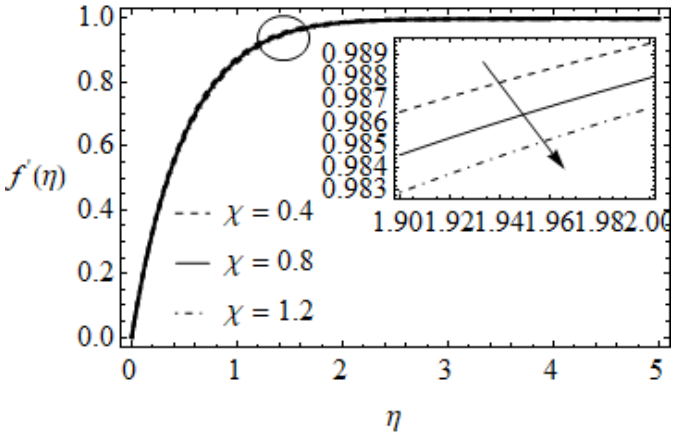

Fig 10. The variation of χ w.r.t. $f'(\eta)$

Table 1. The $\widehat{Re}_x^{1/2}\,\widehat{C}_f$ values for varying δ, α, M, β *and* χ.

δ	α	M	β	χ	$\widehat{Re}_x^{1/2}\,\widehat{C}_f$
0.2					1.7264
0.4					1.8466
0.6					1.9638
0.4	0.5				1.8466
	1				1.7321
	1.5				0.4549
	0.5	1			1.8466
		2			2.1540
		3			2.4027
		1	0.5		1.5486
			1		1.8466
			1.5		2.1524
			1	0.4	1.8466
				0.8	1.8680
				1.2	1.8980

Table 2. The $\widehat{Nu}_x\,\widehat{Re}_x^{-1/2}$ and $\widehat{Sh}_x\,\widehat{Re}_x^{-1/2}$ values for varying χ, *Ra*, *Pr*, *Sc*, *Dr*, *and Sr*

χ	Ra	Pr	Sc	Dr	Sr	$\widehat{Nu}_x\,\widehat{Re}_x^{-1/2}$	$\widehat{Sh}_x\,\widehat{Re}_x^{-1/2}$
0.4	1	6	4	0.2	0.3	0.7315	-0.1378
0.6						0.8353	-0.0764
1.2						0.9945	0.0093
0.4	0.5					0.7315	-0.1378
	1					0.7519	-0.2366
	1.5					0.7617	-0.2768
	1	6.2				0.7430	-0.2463
		7.2				0.6977	-0.2935
		8.2				0.6517	-0.3389
		6	5			0.7519	-0.3247
			6			0.7519	-0.4082
			7			0.7519	-0.4870
			4	0.2		0.7519	-0.2366
				0.4		0.1840	-0.4784
				0.6		0.0284	-0.2366
				0.2	0.2	0.7519	-0.1578
					0.4	0.7519	-0.3155
					0.6	0.7519	-0.4733

non-linear ODEs via similarity variables and are tackled by utilizing Homotopy Analysis Method. The main outcomes for the pertinent parameters are observed from the study are mentioned. The velocity profile decays with mounting values of fluid parameters parameters by increasing significantly enlarge the velocity profile. Hiking values of wedge angle variable On the other hand, cand tenhanced with larger values of Dufour parameter Soretparameter respectively. The thermal field intensified with larger values of parameter skin friction enlarged enhancing values of magnetic, wedge angle and melting parameters. The Sherwood and Nusselt numbers decayed with enhancing values of Soret parameter, Prandtl number, Dufour parameter, Schmidt number.

7 Acknowledgement:

One of the authors Umadevi K B would like to thank the financial assistance received from the "University Grant Commission" below the program of National fellowship for higher education: 201920-NFST-KAR-01277.

References

1) Hsu CH, Tsai TH, Chang CC, Huang WH. A boundary layer flow analysis of a magnetohydrodynamic fluid over a shrinking sheet. *Advances in Mechanical Engineering*. 2019;11(3):168781401983506–168781401983506. Available from: https://dx.doi.org/10.1177/1687814019835069.
2) Ullah H, Khan I, Fiza M, Nawaf N, Hamadneh, Fayz-Al-Asad M, et al. MHD boundary layer flow over a stretching sheet: A New Stochastic Method. *Mathematical Problems in Engineering Volume*. 2021;p. 1–26. Available from: https://doi.org/10.1155/2021/9924593.
3) Berrehal H. Thermodynamics second law analysis for MHD boundary layer flow and heat transfer caused by a moving wedge. *Journal of Mechanical Science and Technology*. 2019;33(6):2949–2955. Available from: https://dx.doi.org/10.1007/s12206-019-0542-4.
4) Mahabaleshwar US, Nagaraju KR, Sheremet MA, Kumar PNV, Lorenzini G. Effect of Mass Transfer and MHD Induced Navier's Slip Flow Due to a non Linear Stretching Sheet. *Journal of Engineering Thermophysics*. 2019;28(4):578–590. Available from: https://dx.doi.org/10.1134/s1810232819040131.
5) Kumar KA, Sugunamma V, Sandeep N. Influence of viscous dissipation on MHD flow of micropolar fluid over a slendering stretching surface with modified heat flux model. *Journal of Thermal Analysis and Calorimetry*. 2020;139(6):3661–3674. Available from: https://dx.doi.org/10.1007/s10973-019-08694-8.
6) De P. Soret-Dufour Effects on Unsteady Flow of Convective Eyring-Powell Magneto Nanofluids over a Semi-Infinite Vertical Plate. *BioNanoScience*. 2019;9(1):7–12. Available from: https://dx.doi.org/10.1007/s12668-018-0583-7.
7) Vafai K, Khan AA, Fatima G, Sait SM, Ellahi R. Dufour, Soret and radiation effects with magnetic dipole on Powell-Eyring fluid flow over a stretching sheet. *International Journal of Numerical Methods for Heat & Fluid Flow*. 2021;31(4):1085–1103. Available from: https://dx.doi.org/10.1108/hff-06-2020-0328.
8) Alao FI. Soret and Dufour Effects on Heat and Mass Transfer of Boundary Layer Flow over Porous Wedge with Thermal Radiation: Bivariate Spectral Relaxation Method. *American Journal of Chemical Engineering*. 2019;7(1):7–7. Available from: https://dx.doi.org/10.11648/j.ajche.20190701.12.
9) Shamshuddin MD, Chamkha AJ, Thumma T, Raju MC. Computation of unsteady MHD mixed convective heat and mass transfer in dissipative reactive micropolar flow considering Soret and Dufour effects. *Frontiers in Heat and Mass Transfer*. 2018;10:1–15. Available from: https://dx.doi.org/10.5098/hmt.10.15.

10) Sarkar S, Endalew MF. Effects of melting process on the hydromagnetic wedge flow of a Casson nanofluid in a porous medium. *Boundary Value Problems*. 2019;2019(1):1–14. Available from: https://dx.doi.org/10.1186/s13661-019-1157-5.
11) Khan MI, Alzahrani F. Dynamics of viscoelastic fluid conveying nanoparticles over a wedge when bioconvection and melting process are significant. *International Communications in Heat and Mass Transfer*. 2021;128:105604–105604. Available from: https://dx.doi.org/10.1016/j.icheatmasstransfer.2021.105604.
12) Humane PP, Patil VS, Patil AB. Chemical reaction and thermal radiation effects on magnetohydrodynamics flow of Casson–Williamson nanofluid over a porous stretching surface. *Proceedings of the Institution of Mechanical Engineers, Part E: Journal of Process Mechanical Engineering*. 2021;235(6):2008–2018. Available from: https://dx.doi.org/10.1177/09544089211025376.
13) Mahabaleshwar US, Anusha T, Sakanaka PH, Bhattacharyya S. Impact of Inclined Lorentz Force and Schmidt Number on Chemically Reactive Newtonian Fluid Flow on a Stretchable Surface When Stefan Blowing and Thermal Radiation are Significant. *Arabian Journal for Science and Engineering*. 2021;46(12):12427–12443. Available from: https://dx.doi.org/10.1007/s13369-021-05976-y.
14) Kumar KA, Sugunamma V, Sandeep N. Effect of thermal radiation on MHD Casson fluid flow over an exponentially stretching curved sheet. *Journal of Thermal Analysis and Calorimetry*. 2020;140(5):2377–2385. Available from: https://dx.doi.org/10.1007/s10973-019-08977-0.
15) Hussain M, Ali A, Ghaffar A, Inc M. Flow and thermal study of MHD Casson fluid past a moving stretching porous wedge. *Journal of Thermal Analysis and Calorimetry*. 2021. Available from: https://dx.doi.org/10.1007/s10973-021-10983-0.
16) Kumar KA, Ramadevi B, Sugunamma V, Reddy JVR. Heat transfer characteristics on MHD Powell-Eyring fluid flow across a shrinking wedge with non-uniform heat source/sink. *Journal of Mechanical Engineering and Sciences*. 2019;13(1):4558–4574. Available from: https://dx.doi.org/10.15282/jmes.13.1.2019.15.0385.